Multichannel phase-shifted interferometer

Osuk Y. Kwon

Electro-Optics Laboratory, Lockheed Palo Alto Research Laboratory, Palo Alto, California 94304

Received September 26, 1983; accepted November 21, 1983

A new real-time interferometer based on diffraction phenomena is discussed. It consists of a point-diffraction interferometer fabricated on a transmission grating. The real-time data-analysis capability is achieved by simultaneously introducing a phase shift (piston) on the three separate channels of diffracted interferograms. Mathematical analysis and preliminary observational results are included.

A real-time interferometric system is introduced that is simple to use and has the capability of a high data-processing rate with comparable measurement accuracies. This new interferometer eliminates the need for electro-optical devices, auxilliary waveplates, polarizers, or rotating elements, which are used in most other real-time interferometric systems.[1–6] The basic operational principle of this new interferometric technique involves (1) self-referencing the test wave front to a diffracted spherical reference wave front and (2) using a transmissive diffraction grating to generate phase-shifted interferograms simultaneously for instantaneous heterodyne measurement and analysis.

There are many ways of transforming the conventional (stationary) interferometers into real-time (dynamic) interferometers. One of the methods is phase-shifting interferometry.[7,8] In general, the intensity distribution of an interference pattern can be written at each detector point as

$$I(x,y) = I_a + I_b \cos[\Phi(x,y) + \delta], \tag{1}$$

where there are basically three unknowns, the average intensity I_a, the modulation intensity I_b, and the wave-front phase $\Phi(x, y)$. δ is an arbitrary constant phase difference between the object and reference wave fronts. The simplest solution for $\Phi(x, y)$ can be obtained by using three phase steps starting at $\delta = \pi/4$ with increments of $\pi/2$:

$$\begin{aligned} I_A(x,y) &= I_a + I_b \cos[\phi(x,y) + \pi/4], \\ I_B(x,y) &= I_a + I_b \cos[\phi(x,y) + 3\pi/4], \\ I_C(x,y) &= I_a + I_b \cos[\phi(x,y) + 5\pi/4]. \end{aligned} \tag{2}$$

The final expression for $\phi(x, y)$ is then written as

$$\phi(x,y) = \tan^{-1}\left[\frac{I_C(x,y) - I_B(x,y)}{I_A(x,y) - I_B(x,y)}\right]. \tag{3}$$

The new interferometer operates based on a principle similar to that of the phase-shifting method. The phase shifting is obtained by introducing a transmissive grating to the substrate of a point-diffraction interferometer (PDI),[9,10] as illustrated in Fig. 1.

A similar Fourier method[11] is used to find the resultant intensity distributions at the image plane. The amplitude-transmittance function for the new interferometer can be expressed mathematically as

$$t(x,y) = t_p(x,y)t_g(x,y), \tag{4}$$

where the amplitude transmittance of an ordinary PDI is written as

$$t_p(x,y) = t_b + (1 - t_b) \times \mathrm{cyl}\left\{\frac{[(x - x_0)^2 + (y - y_0)^2]^{1/2}}{d}\right\}, \tag{5}$$

which represents a partially transmitting plane of amplitude transmittance t_b, with a totally transparent circular pinhole of diameter d, shifted from the origin by (x_0, y_0). The amplitude transmittance of the diffraction grating is written as

$$t_g(x,y) = \tfrac{1}{2}[1 + \beta \cos 2\pi\xi(x - x_g)], \tag{6}$$

where an amplitude cosinusoidal transmissive grating of diffraction efficiency, $\beta^2/4$, and a spatial frequency of ξ are assumed. x_g represents the relative position of the center of the pinhole in the PDI within one period of grating. The relative pinhole position is the critical source of the simultaneous phase shift in the resultant interferograms, which is shown below. The grating needs to have a proper value of spatial frequency in order to achieve separated pupils of different diffracted orders, i.e.,

$$\xi > 1/(2\lambda F) \quad \text{or} \quad d_g < 2\lambda F, \tag{7}$$

where λ is the operational wavelength, $d_g = 1/\xi$ is

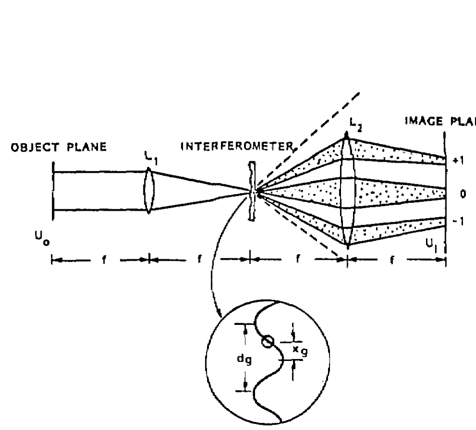

Fig. 1. Optical schematic of the new multichannel phase-shifted interferometer with magnified view of the relative pinhole position within a period of substrate grating.

0146-9592/84/020059-03$2.00/0

the grating period, and F is the aperture ratio of the focused object beam.

The complex amplitude of the object wave front is written as

$$U_0(x, y) = \mathrm{cyl}\left[\frac{(x^2 + y^2)^{1/2}}{D}\right]\exp\left[\frac{i2\pi}{\lambda}\, W(x, y)\right], \tag{8}$$

where D is the diameter of the object wave front at L_1 and $W(x, y)$ is the optical path difference of the test wave front.

Assuming unit magnification and neglecting an unimportant quadratic propagation phase factor across the image, the resultant complex amplitude in the image plane is given by

$$\begin{aligned} U_i(x, y) = {} & t_b\, \mathrm{cyl}\left[\frac{(x^2 + y^2)^{1/2}}{D}\right] \exp[i\phi(x, y)] \\ & + \frac{1}{2} t_b\beta\, \mathrm{cyl}\left\{\frac{[(x - s)^2 + y^2]^{1/2}}{D}\right\} \\ & \times \exp[i\phi(x, y)] \exp(-i2\pi\xi x_g) \\ & + \frac{1}{2} t_b\beta\, \mathrm{cyl}\left\{\frac{[(x + s)^2 + y^2]^{1/2}}{D}\right\} \\ & \times \exp[i\phi(x, y)] \exp(i2\pi\xi x_g) \\ & + (1 - t_b)\alpha[1 + \beta \cos 2\pi\xi(x_0 - x_g)] \\ & \times \exp[-i2\pi(x_0 x + y_0 y)/\lambda f], \end{aligned} \tag{9}$$

where

$$\phi(x, y) = (2\pi/\lambda) W(x, y).$$

The first three terms represent object beams: the undiffracted (zeroth), plus-first, and minus-first orders. Notice that the zeroth-order term is exactly the same as the one encountered in the conventional PDI, and the pupils of first-order terms are translated by $s = \lambda f\xi$ across the perpendicular direction of the grating with an additional phase (piston) term of

$$\Delta\phi_{\pm} = \pm 2\pi\xi x_g. \tag{10}$$

The last term represents the global spherical reference wave front with associated magnitude and tilt terms, which interfere with the three object beams simultaneously to produce the three interferograms with constant phase shift in tandem (α is a constant from the convolution operation).

The final expressions for the intensity distributions of the interferograms are rewritten as

$$\begin{aligned} I_-(x, y) &= I_1^{(-)} + I_2^{(-)} \cos[\phi(x, y) - 2\pi\xi x_g], \\ I_0(x, y) &= I_1^{(0)} + I_2^{(0)} \cos[\phi(x, y)], \\ I_+(x, y) &= I_1^{(+)} + I_2^{(+)} \cos[(x, y) + 2\pi\xi x_g], \end{aligned} \tag{11}$$

where

$$I_1^{(-)} = I_1^{(+)} = I_1,$$

$$I_2^{(-)} = I_2^{(+)} = I_2,$$

and

$$I_1^{(0)} = I_1 + \left(1 - \frac{\beta^2}{4}\right) t_b{}^2,$$

$$I_2^{(0)} = \frac{2}{\beta} I_2.$$

Again, the simplest solution for $\phi(x, y)$ is obtained when the phase shift $\Delta\phi = 2\pi\xi x_g = \pi/2$ and can be written as

$$\phi(x, y) = \tan^{-1} \times \left\{\frac{I_- - I_+}{\beta\left[\frac{2I_0 - (I_- + I_+)}{2} + \left(1 - \frac{\beta^2}{4}\right) t_b{}^2\right]}\right\}. \tag{12}$$

Preliminary laboratory observations of the instantaneously phase-shifted interferograms were achieved. First an ordinary PDI was proximately contacted with a phase grating, and sets of three interferograms with variable phase shift were demonstrated by continuously translating the grating with respect to the fixed PDI pinhole position. Later, many PDI's were fabricated on the holographically made grating on a Kodak 649F plate. Many pinholes can be fabricated by using small microballoons as maskings. The balloons are spread over the grating plate and a thin layer (a few hundred angstroms thick) of aluminum coating is overcoated; then the microballoons are removed by an air jet, thus leaving pinholes in the coating. Figure 2 shows the typical results of the fabricated pinholes and their corresponding three phase-shifted interferograms. In this example, the grating has 20-μm line spacing, and the diameter of the pinholes is 5 μm. The beam ratio of the test beam is $F/20$.

Figure 2(a) demonstrates that the pinhole located at $x_g = d_g/4$ produces three interferograms with a relative phase shift of 90°. The results shown in Figs. 2(b) and 2(c) are not useful for the purpose of phase-shifted interferometry but clearly illustrate and prove the principles of this new interferometer. If $x_g = 0$, then $\Delta\phi = 0$, that is, the three interferograms are identical [Fig. 2(b)]. If $x_g = d_g/2$, then $\Delta\phi = \pi$; then ± first-order

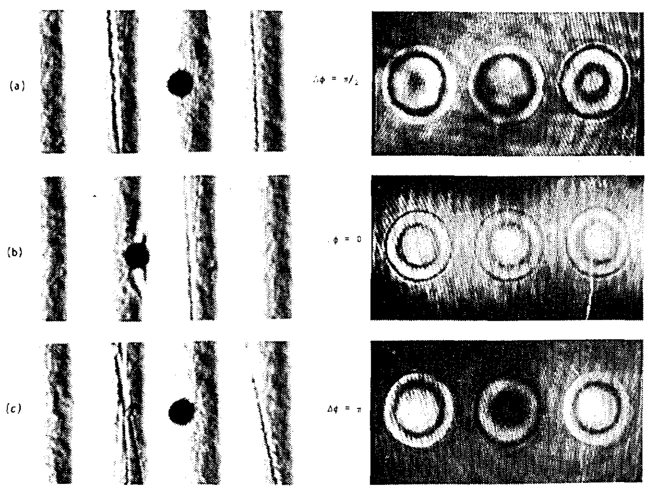

Fig. 2. Microscopic photographs of pinholes and corresponding interferograms for $F/20$ object beams. The diameter of the pinholes is 5 μm, and the grating spacing is 20 μm. (a) $X_g = d_g/4$ ($\Delta\phi = \pi/2$). (b) $X_g = 0$ ($\Delta\phi = 0$). (c) $X_g = d_g/2$ ($\Delta\phi = \pi$).

interferograms are identical but conjugate to zeroth-order fringe [Fig. 2(c)].

The basic analysis and experimental verification of the principles of a new multichannel diffraction interferometer have been presented. The interferometer is based on the diffraction properties of a grating and a pinhole. The parallel nature of the phase shifting can speed up the data-processing rate faster than other types of interferometers for use in systems that require a high frame rate of pulsed sources by introducing three parallel detector channels. The simplicity in the design and operation is evident: Various optical or electro-optical phase-shifting components are eliminated that are required in most other types of real-time interferometers. This can be a great advantage, especially for use in other wavelengths of interest, because of the problems of availability, complexity, and the high cost of proper optical and electro-optical materials. However, this interferometer has rather low efficiency in the use of the power in the object beam similar to the ordinary PDI and is limited to a slower beam ratio. Also, more-elaborate detector calibration is required because of the multichannel aspect. In other words, this new interferometer greatly simplifies the optic portion of the heterodyne interferometry by imposing tolerable burdens on the detector and electronics as a common-path self-referencing interferometer for simple, compact, stable, and higher-speed operation for both continuous- and pulsed-mode operations.

References

1. R. K. Crane, Appl. Opt. **8,** 538 (1969).
2. D. Malacara, I. Rizo, and P. L. Morales, Appl. Opt. **8,** 1746 (1969).
3. W. H. Stevenson, Appl. Opt. **9,** 649 (1970).
4. J. H. Bruning, D. R. Harriott, J. E. Gallagher, D. P. Rosenfeld, A. D. White, and D. J. Brangaccio, Appl. Opt. **13,** 2693 (1974).
5. G. E. Sommargren, J. Opt. Soc. Am. **65,** 960 (1975).
6. J. W. Hardy, J. E. Lefebvre, and C. L. Koliopoulos, J. Opt. Soc. Am. **67,** 360 (1977).
7. J. C. Wyant, Appl. Opt. **14,** 2622 (1975).
8. J. C. Wyant, Laser Focus **65**(5), 65 (1982).
9. R. N. Smartt and J. Strong, J. Opt. Soc. Am. **62,** 737 (1972).
10. R. N. Smartt and W. H. Steel, Jpn. J. Appl. Phys. Suppl. 1 **14,** 351 (1975).
11. C. Koliopoulos, O. Kwon, R. Shagam, J. C. Wyant, and C. R. Hayslett, Opt. Lett. **3,** 118 (1978).